STEM CELLS®

REGENERATIVE MEDICINE

# Derivation of Mesenchymal Stem Cells from Human Induced Pluripotent Stem Cells Cultured on Synthetic Substrates

L.G. VILLA-DIAZ,[a] S.E. BROWN,[a] Y. LIU,[b] A.M. ROSS,[c] J. LAHANN,[c] J.M. PARENT,[b,d] P.H. KREBSBACH[a]

[a]Department of Biologic & Materials Sciences, School of Dentistry, [b]Department of Neurology, Medical School, [c]Department of Chemical Engineering, and [d]Neurology Service, Veterans Administrator Ann Arbor Healthcare System, University of Michigan,
Ann Arbor, Michigan, USA

**Key Words.** Induced pluripotent stem cells • Mesenchymal stem cells • Bone • Xenogeneic-free culture • Regeneration

ABSTRACT

**Human-induced pluripotent stem cells (hiPSCs) may represent an ideal cell source for research and applications in regenerative medicine. However, standard culture conditions that depend on the use of undefined substrates and xenogeneic medium components represent a significant obstacle to clinical translation. Recently, we reported a defined culture system for human embryonic stem cells using a synthetic polymer coating, poly[2-(methacryloyloxy)ethyl dimethyl-(3-sulfopropyl)ammonium hydroxide] (PMEDSAH), in conjunction with xenogeneic-free culture medium. Here, we tested the hypothesis that iPSCs could be maintained in an undifferentiated state in this xeno-free culture system and subsequently be differentiated into mesenchymal stem cells (iPS-MSCs). hiPSCs were cultured on PMEDSAH and differentiated into functional MSCs, as confirmed by expression of characteristic MSC markers (CD166+, CD105+, CD90+,CD73+, CD31−, CD34−, and CD45−) and their ability to differentiate in vitro into adipogenic, chondrogenic, and osteoblastic lineages. To demonstrate the potential of iPS-MSCs to regenerate bone in vivo, the newly derived cells were induced to osteoblast differentiation for 4 days and transplanted into calvaria defects in immunocompromised mice for 8 weeks. MicroCT and histologic analyses demonstrated de novo bone formation in the calvaria defects for animals treated with iPS-MSCs but not for the control group. Moreover, positive staining for human nuclear antigen and human mitochondria monoclonal antibodies confirmed the participation of the transplanted hiPS-MSCs in the regenerated bone. These results demonstrate that hiPSCs cultured in a xeno-free system have the capability to differentiate into functional MSCs with the ability to form bone in vivo.** STEM CELLS *2012;30:1174–1181*

Disclosure of potential conflicts of interest is found at the end of this article.

## INTRODUCTION

Induced pluripotent stem cells (iPSCs) and embryonic stem cells (ESCs) have the ability to undergo self-renewal and differentiate into every cell type in the body [1–3], and therefore represent a potential renewable cell source for cell therapies and regenerative medicine. Both pluripotent stem cell sources can further give rise to progenitor cells, such as mesenchymal stem cells (MSCs) that can differentiate into mesodermal derivatives, such as bone, fat, cartilage, tendon, and muscle [4–6]. In addition, MSCs have important immunomodulatory and engraftment-promoting properties [7]. While MSCs can be isolated from bone marrow [8], adipose tissue [9, 10], umbilical cord blood [11], umbilical cord stroma [12], placenta [13], and other tissues and organs, the harvesting procedures are invasive, expensive, and laborious. Direct derivation of MSCs from pluripotent stem cells represents an effective alternative to obtain larger population of progenitor cells that are needed for cell therapies or regenerative medicine.

Like human ESCs (hESCs), human iPSCs (hiPSCs) will need to be cultured in clinically compliant conditions if broader translation into clinical practice is intended. Although coculture with human feeder cells represent a xeno-free option for the in vitro expansion of pluripotent stem cells [14], such human feeder cell environments are undefined, may contain pathogens, and will require expensive and labor-intensive screening. Similarly, extracellular matrix coatings made of undefined animal-derived proteins such as Matrigel, vitronectin, fibronectin, or laminin are also expensive, may be immunologically incompatible with humans, have batch to batch variation, and will require extensive pretransplantation screening.

Author contributions: L.G.V.-D.: conception and design, collection and/or assembly of data, data analysis and interpretation, manuscript writing, and final approval of manuscript; S.E.B.: collection and/or assembly of data, data analysis and interpretation, and final approval of manuscript; Y.L.: provision of study material, collection and/or assembly of data, data analysis and interpretation, manuscript writing, and final approval of manuscript; A.M.R. and J.L.: provision of study material and final approval of manuscript; J.M.P.: financial support, provision of study material, and final approval of manuscript; P.H.K.: conception and design, financial support, data analysis and interpretation, and final approval of manuscript.

Correspondence: P.H. Krebsbach, D.D.S., Ph.D., Department of Biologic and Materials Sciences, School of Dentistry, University of Michigan, 1011 North University Ave, Ann Arbor, Michigan 48109, USA. Telephone: (734)-936-2600; Fax: (734)-647-2110; e-mail: paulk@umich.edu Received August 10, 2011; accepted for publication February 19, 2012; first published online in STEM CELLS *EXPRESS* March 13, 2012.  1066-5099/2012/$30.00/0 doi: 10.1002/stem.1084

To overcome some of the limitations of human feeder cells or animal-derived extracellular matrices, synthetic cell culture substrates for pluripotent stem cells that are devoid of xenogeneic components have recently been developed [15–20]. Some of these substrates are based on recombinant proteins or peptides and thus are hampered by well-known problems of polypeptide matrices such as difficulties in sterilization, propensity to degrade [21], and the high cost of production [22].

Alternatively, cell culture coatings based on synthetic polymers can be reproducibly fabricated, are inexpensive, and are amenable to chemical modification, and thus represent a valuable option to expand pluripotent stem cells. Recently, we reported the development of a fully defined synthetic polymer coating made of poly[2-(methacryloyloxy)ethyl dimethyl-(3-sulfopropyl)ammonium hydroxide] (PMEDSAH), which in combination with human cell-conditioned or chemically defined medium supports the long-term culture and self-renewal of undifferentiated hESCs [20, 23]. This pluripotent culture system makes use of a synthetic polymer as the structural motifs in cell-substrate interactions (i.e., no peptides, sugars, or proteins) and therefore provides a unique xenogeneic-free environment.

In this study, we tested the hypothesis that human iPSCs can continuously proliferate (15 passages) on PMEDSAH in an undifferentiated state and yet remain capable of subsequent lineage-specific differentiation. Importantly, we also demonstrate that hiPSCs cultured in this clinically compliant culture system can be directed toward differentiation into functional MSCs in vitro and bone formation in vivo.

## Materials and Methods

### Generation of iPSCs

Retroviral vectors carrying *Klf4, Sox2, Oct3/4*, and *c-Myc* were generated by transient cotransfection (Addgene Cambridge, MA; http://www.adgene.org plasmids 17217, 17219, 17220, and 17226, and VSV-g envelope plasmid 8454) into Clontech (Mountain View, CA; http://www.clontech.com) GP2-293 packaging cells. Viral supernatant was harvested after 60 hours, filtered, and concentrated. Human fibroblasts were cultured in Dulbecco's modified Eagle's medium (DMEM) + 10% fetal calf serum with 1× nonessential amino acid supplement (NEAA, Invitrogen; Grand Island, NY; http://www.invitrogen.com). To generate iPSCs, two rounds of viral transduction of 30,000 fibroblasts were performed and cells were incubated with virus for 48 hours. After 4 days, cells were passaged on irradiated mouse embryonic fibroblasts (MEFs) in fibroblast medium, and next day switched to hESC medium, consisting of DMEM/F12 (Invitrogen), 20% knockout serum replacer (Invitrogen), 1 mM L-glutamine (Invitrogen), 1× NEAA, 0.1 mM $\beta$-mercaptoethanol (Sigma-Aldrich, St. Louis, MO; http://www.sigmaaldrich.com), and 4 ng/ml human recombinant fibroblast growth factor 2 (FGF2; Invitrogen). Cells were cultured at 37°C/5% $CO_2$. iPS colonies were manually picked and passaged. Immunohistochemistry confirmed expression of Nanog, SSEA4, Oct3/4, and alkaline phosphatase (ALP). Culture of H7-hESCs (WA07, WiCell Research Institute; NIH Registration Number 0061) was performed as described above for hiPSCs.

### Illumina Microarray

Total RNA was purified from iPSCs, parental fibroblasts, and H7-hESCs with RNeasy Mini kit (Qiagen; Valencia, CA; http://www.qiagen.com) and DNase-I treatment. A total of 400 ng of RNA was amplified and labeled with Total Prep RNA amplification kit (Ambion; Grand Island, NY; http://www.invitrogen.com), and 750 ng of biotin-labeled cRNA was used to hybridize Illumina HumanHT-12 v4 Expression BeadChip (Illumina, Inc, San Diego, CA; http://illumina.com). After washing, chips were coupled with Cy3 and scanned in an Illumina BeadArray Reader (Illumina, Inc.). Un-normalized summary probe profiles, with associated probe annotation, were output from BeadStudio.

### Culture of iPSCs in Xeno-Free Culture Conditions

iPSCs were cultured on PMEDSAH-coated plates with human-cell-conditioned medium (hCCM, GlobalStem, Inc.; Rockville, MD; http://www.globalstem.com) supplemented with 4 ng/ml of FGF2, as described previously [20, 23]. PMEDSAH-coated plates were preincubated with hCCM for at least 48 hours at 37°C in 5% $CO_2$ before use. Twenty-four hours before passaging onto PMEDSAH-coated plates, hESC medium was replaced with hCCM and passaged mechanically using a sterile pulled-glass pipette. Cells were observed every 48 hours using a Leica stereomicroscope, and differentiated cells were removed mechanically, followed by replacement of cell culture medium.

### Derivation, Culture, and Characterization of MSCs

To induce differentiation of iPSCs into MSCs, embryoid bodies (EBs) were formed and cultured in suspension for 7 days with hCCM in low-attachment culture dishes. Approximately 70 EBs were plated onto 0.1% gelatin-coated dishes in growth medium (alpha minimum essential medium: $\alpha$-MEM, 10% fetal bovine serum: (FBS), 200 mM L-glutamine and 10 mM NEAA). Cells growing from these EBs were cultured for up to 2 weeks to reach confluence and passaged until a homogeneous fibroblastic morphology appeared. In subsequent culture, cells were seeded at a density of $7 \times 10^3/cm^2$.

### Colony-Forming Unit Assay

To determine the existence of progenitors in the iPSC-MSC-derived population, the colony-forming units assay was performed. Briefly, 300 and 600 iPS-MSCs at passage 4 were seeded per well of a six-well plate and cultured in growth medium for 12 days. After three washes with phosphate-buffered saline (PBS), cells were fixed and stained with a 0.5% crystal violet-methanol solution for 30 minutes. The assay was performed in triplicate.

### Cell Doubling Time

The cell doubling time was calculated using the algorithm provided by http://www.doubling-time.com/compute.php, with an initial seeding of $7 \times 10^3$ cells per well and evaluated at 6, 24, and 48 hours postseeding. The assay was performed in triplicate.

### Flow Cytometry Analysis

Cell surface antigen profiling was performed using fluorescence-activated cell sorting (FACS). Derived iPS-MSCs were harvested using trypsin 0.25% EDTA, and single cell suspensions were washed in cold bovine serum albumin (BSA) 0.5% (wt/vol) in Dulbecco's phosphate-buffered saline (DPBS) and incubated at a concentration of $1 \times 10^6$ cells per milliliter in 1 $\mu$g/ml unconjugated goat anti-human IgG (Invitrogen) on ice for 15 minutes, to block nonspecific protein binding. Samples ($2.5 \times 10^5$ cells) were incubated on ice with optimal dilution of fluorochrome-conjugated monoclonal antibodies (mAbs) in dark, and to further control for nonspecific detection, control samples were incubated with phycoerythrin (PE) mouse immunoglobulin G1 (IgG1) $\kappa$ isotype control and FITC mouse IgG $\kappa$ isotype control. All mAbs and isotype controls were of the IgG1 isotype and from BD Biosciences (San Jose, CA; http://www.bdbiosciences.com) except for CD105, which was from eBioscience (San Diego, CA; http://

ebiosciences.com). The following conjugated antibodies were used: fluorescein isothiocyanate (FITC)-conjugated against CD90, and CD45, PE-conjugated against CD29, CD31, CD34, CD49e, CD73, CD105, and CD166. After 30 minutes incubation, cells were washed twice with ice cold 0.5% BSA/DPBS. At least 10,000 events were acquired for each sample using a FACSCalibur instrument (BD Biosciences) and cell flow cytometry data were analyzed using CELLQUEST software (BD Biosciences). Human bone marrow stromal cells and human vascular endothelial cells were analyzed by flow cytometry as controls.

## Differentiation Assays

For functional differentiation, MSCs at passages 6 and 7 were used. For osteogenesis, cells were incubated in α-MEM with 10% fetal calf serum (FCS), 100 U/ml penicillin, 100 μg/ml streptomycin, 2 mM L-glutamine, 10 mM β-glycerophosphate (Sigma), 100 nM dexamethasone (Sigma), and 50 μM ascorbate-2-phosphate (Sigma). Media were changed two times per week for 3 weeks. Cells were fixed with 10% formalin for 20 minutes at RT and stained with Alizarin Red, pH 4.1 for 20 minutes at RT.

For adipogenesis, cells were incubated in DMEM with 15% fetal calf serum (FCS), 100 U/ml penicillin, 100 μg/ml streptomycin, 12 mM L-glutamine, 5 μg/ml insulin (Sigma), 50 μM indomethacin (Sigma), $1 \times 10^{-6}$ M dexamethasone (Sigma), and 0.5 μM 3-isobutyl-1-methylxanthine (Sigma). Media were changed two times per week for 3 weeks. Cells were fixed with 10% formalin for 20 minutes at RT and stained with Oil Red (Sigma) in ethanol for 20 minutes at RT.

Chondrogenic differentiation was induced by culturing $2 \times 10^6$ iPS-MSCs in pellets. Cells were suspended in 2 ml of chondrogenic medium in 15 ml centrifugation tubes and centrifuged at 600*g* for 5 minutes and cultured for 21 days. Medium was changed every 3 days and consisted of high-glucose DMEM (Gibco; Grand Island, NY; http://www.invitrogen.com) with 10% FBS (Gibco), 100 mM sodium pyruvate, 40 μg/ml proline, 100 nM dexamethasone, 200 μM ascorbic acid (all from Sigma), and 10 ng/ml transforming growth factor (TGF)-β3 (R&D systems; Minneapolis, MN; http://www.RnDSystem.com). Cells were fixed with 10% formalin for 20 minutes at RT and stained Safranin O (Sigma) in ethanol for 20 minutes at RT.

## Preparation of iPS-MSCs for Implantation

iPS-MSCs at passage 4 were harvested using 0.25% trypsin-0.53 mM EDTA (Gibco) and were resuspended in 5 mg/ml human plasma fibrinogen (Sigma) at a concentration of $2 \times 10^6$ cells per 40 μl. Fibrinogen-cell suspension was then pipetted directly into $6 \times 3$ mm$^2$ cubic pieces of Gelfoam (Pharmacia & Upjohn Co.; Pfizer Inc, NY, NY; http://www.pfizer.com), followed by 5 μl of human thrombin (200 U/ml; Sigma). Gelation of fibrin was observed and placed immediately on ice until implantation.

## Surgical Procedure and Cell Transplantation in Craniofacial Defect Model

All procedures were approved by the University of Michigan Committee on the Use and Care of Animals. Five-week-old female immunocompromised mice (N:NIH-bg-*v*-xid; Harlan Sprague Dawley, Inc.) were anesthetized with intraperitoneal injections of ketamine (Ketaset, 75 mg/kg, Fort Dodge Animal Health Pfizer Inc, NY, NY; http://www.pfizer.com) and xylazine (Ansed, 10 mg/kg, Lloyd laboratories, Walnut, CA; http://www.lloydlab.com). A semilunar scalp incision was made from right to left in the postauricular area, and a full-thickness flap was elevated. Periosteum overlying the calvarial bone was completely resected. A trephine was used to create a 5-mm craniotomy defect centered on the sagittal sinus, and the calvarial disk was removed. One gelfoam sponge with or without hiPS-MSCs was inserted in the calvaria defect per animal. Incisions were closed with 4-0 Chromic Gut suture (Ethicon/Johnson&-Johnson, Somerville, NJ; http://www.ethicon.com). All mice were killed 8 weeks after implantation.

## Radiology, Histology, and MicroCT Analyses

Radiographic analysis was performed using a microradiographic apparatus (Faxitron Bioptics, LLC; Tucson, AR; http://www.faxitron.com). MicroCT was used to quantify bone volume (BV) and mineral density of the newly formed bone within the 5-mm diameter craniotomy defect. Calvaria were fixed in Z fix (Anatech LTD, Battle Creek, MI; http://anatechltusa.com), embedded in 1% agarose, placed in a 34 mm diameter tube, and scanned over the entire length of calvaria using a microCT system (μCT100 Scanco Medical, Wayne, PA; http://www.scanco.ch). Scan settings were: voxel size 12 μm, medium resolution 70 kVp, 114 μA, 0.5 mm Al filter, and integration time 500 microsecond. The center of the defect was visually identified and a cylindrical volume of interest (5-mm diameter) was drawn centered around the defect. Analysis was performed using manufacturer's evaluation software and a fixed global threshold of 23% (230 on a grayscale of 0–1,000) was used to segment bone from non-bone. Total BV (mm$^3$) and tissue mineral density of bone (D) were computed and calibrated to the manufacturer's hydroxyapatite phantom.

For histological analysis, calvaria were decalcified with a 10% EDTA solution for 2 days, dehydrated with gradient alcohols, and embedded in paraffin. Coronal sections 5 μm in thickness were cut and stained with hematoxylin and eosin. Sections were deparaffinized and rehydrated, followed by antigen retrieval treatment, blockage of endogenous peroxidase, 2.5% horse serum and avidin/biotinin. Sections were reacted with mouse anti-human nuclei monoclonal and mouse anti-human mitochondria mAbs (Millipore, Billerica, MA; http://www.millipore.com), and signals were amplified with ImmPRESS reagent (VectorLabs, Burlingame, CA; http://www.verctorlabs.com) and imaged with ImmPACT DAB substrate (VectorLabs).

## Quantitative Real-Time PCR

Total RNA was extracted using Trizol (Invitrogen) and 1 mg of RNA was reverse transcribed into cDNA using Superscript III Reverse Transcriptase (Invitrogen). Two microliters of diluted reverse transcribed cDNA (RT reaction, 1:5 in RNase-free water) was amplified in a 30 μl PCR assay volume, using TaqMan Gene Expression Master Mix (Applied Biosystems, Carlsbad, CA; http://www.appliedbiosystems.com), target primers, and Probe (unlabeled PCR primers and a carboxyfluorescein (FAM) dye-labeled TaqMan minor groove binder probe) (Applied Biosystems). Gene expression was measured by quantitative real-time PCR (qRT-PCR) on an ABI Prism 7700 Sequence Detection System (Applied Biosystems). The relative RNA expression levels of target genes were analyzed by the comparative $C_T$ method using β-actin as an internal control. Subsequently, expression levels of investigated genes were normalized to expression levels of control samples and reported as fold changes. To calculated the fold change in samples with reduction in expression compared to control samples, the following formula was used $= -1/2^{-\Delta\Delta C_T}$ [24].

To detect transgene expression, total RNA was purified from iPSCs passage 25, parental fibroblasts, and infected fibroblasts using the RNeasy Mini kit (Qiagen) and DNase I treatment. First strand cDNA synthesis was performed from 0.5 μg of total RNA using Superscript III reverse transcriptase (Invitrogen) and random hexamers according to manufacturer's instructions. Quantitative PCR (qPCR) was performed with SYBR Green qPCR (PE Applied Biosystems) containing 200 nM each of forward and reverse primers and template using Bio-Rad iCycler PCR machine. The following primer sequences were used: F (aggatcccagtgtggtggta), *POU5F1* (*Oct4*) R (ccttggaagcttagccaggt), *SOX2* R (gcttagcctcgtcgatgaac), *KLF4*

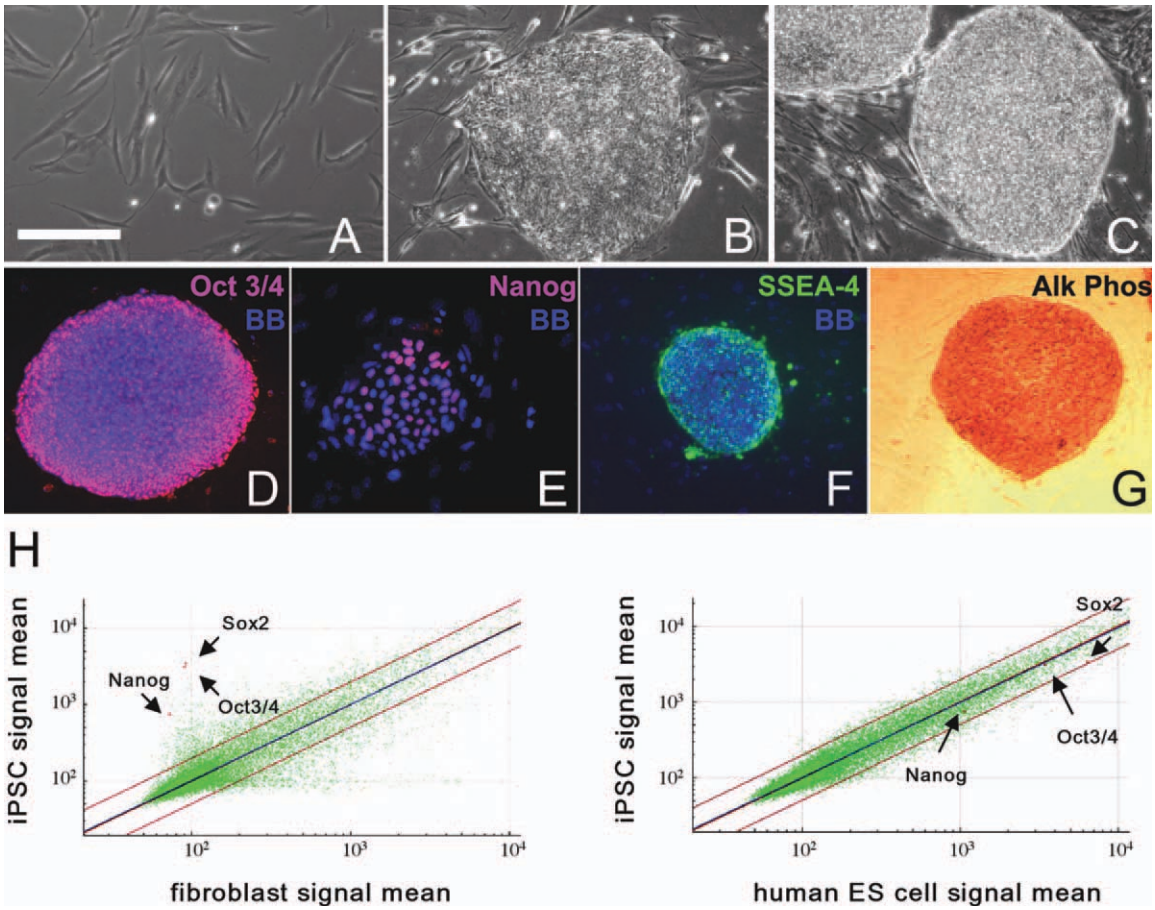


**Figure 1.** Characterization of human iPSCs. Micrograph of parental fibroblasts **(A)**, derived iPS **(B)**, and control human ES colonies **(C)**. iPS colonies expressed Oct3/4 **(D)**, Nanog **(E)**, SSEA4 **(F)**, and alkaline phosphatase **(G)**. Cell nuclei were stained with BB. **(H):** Scatter plots showing global gene expression patterns of cells in (A--C). Pluripotent genes are indicated with red dots. Scale bar = 100 $\mu$m in A and E and 200 $\mu$m in (B–D), (F), and (G). Abbreviations: BB, bisbenzimide; ES, embryonic stem; iPSC, induced pluripotent stem cells.

R (ggtctctctccgaggtaggg), *c-MYC* R (cagcagctcgaatttcttcc), and glyceraldehyde-3-phosphate dehydrogenase (*GAPDH*) as internal control: F (tcgacagtcagccgcatcttcttt) and R (accaaatccgttgactccgacctt).

### Cytogenetic Analysis

Karyotype analysis was performed at Cell Line Genetics (Madison, WI; http://www.clgenetics.com). Chromosomes were prepared using standard protocols and measurements were performed using Giemsa/Trypsin/Leishman (GTL)-banding method on at least 20 metaphase preparations.

### Statistical Analyses

All experiments were performed in triplicate and data were expressed as mean value ± SD and analyzed by unpaired *t* test. Levels of statistical significance were set at $p < .05$.

## Results

### Derivation of iPSCs and Culture in Xeno-Free Conditions

Human dermal fibroblasts were reprogrammed into iPSCs by overexpression of *Oct3/4* (also known as *POU5F1*), *Sox2*, *Klf4*, and *c-Myc* genes individually packaged into retroviral vectors. After 10–14 days in culture on irradiated MEFs, hESC-like colonies are formed and proliferated (Fig. 1A--1C). The morphology of emerging iPSC colonies resembled the distinctive characteristic morphology of undifferentiated hESC colonies with well-defined borders and a high nucleus:cytoplasm ratio [3] (Fig. 1B,1C). Histochemical analysis revealed continuous expression of Oct3/4, Nanog, SSEA4, and ALP (Fig. 1D--1G), while qPCR analysis showed the suppression of transgene RNA expression (supporting information Table 1) in iPSCs after 25 passages, indicating the self-sustaining of the iPSC lines. Global gene expression analysis showed that *Nanog*, *Oct3/4*, and *Sox2* from iPSCs colocalized in scatter plots with the gene expression patterns of H7-hESCs, while differing from the parental skin fibroblast cell line (Fig. 1H), further confirming successful cellular reprogramming.

To establish pluripotent cell cultures in xeno-free conditions, hiPSCs were transitioned to PMEDSAH-coated plates with hCCM, as previously described for hESCs [20, 23]. PMEDSAH-coated plates continuously supported attachment, proliferation, self-renewal, and maintenance of pluripotency of undifferentiated hiPSCs. These findings were confirmed by rigorous characterization performed every five passages, including karyotype analysis (supporting information Fig. 1A), expression of Oct3/4, Sox2, and SSEA4 (Fig. 2), and formation of EBs expressing markers of all three germ layers (data not shown).

### Derivation of MSCs from hiPSCs

The derivation of hiPS-MSCs was performed following protocols used for the differentiation of hESCs into MSCs [5].

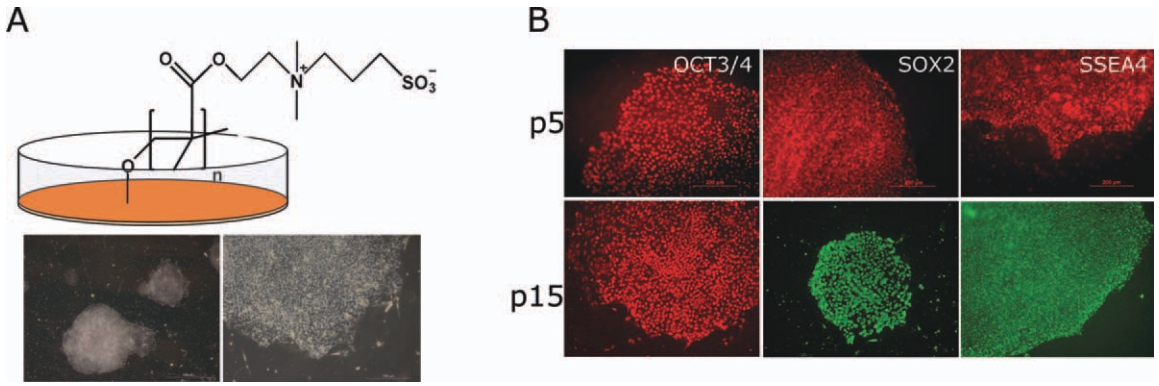


**Figure 2.** Culture of human-induced pluripotent stem cells (iPSCs) in a clinically compliant culture system. **(A):** A schematic representation of poly[2-(methacryloyloxy)ethyl dimethyl-(3-sulfopropyl)ammonium hydroxide] (PMEDSAH)-coated plates and bright-field images of human iPS colonies growing on PMEDSAH with human-cell-conditioned medium. The micrograph image on the left was taken at ×20 in a stereoscope, while the micrograph on the right was taken at ×100 in an inverted microscope. **(B):** Human iPSCs cultured on PMEDSAH at passage (P) 5 and 15 expressing the pluripotent stem cell markers OCT3/4, SOX2, and SSEA4.

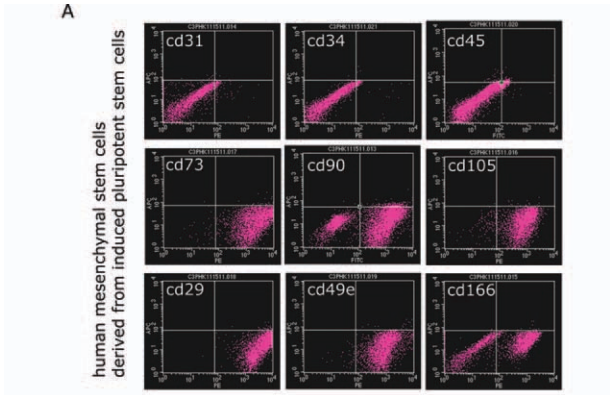


B

| | HUVEC | hBMSC | hiPS-MSCs | | |
|---|---|---|---|---|---|
| | | | p1 | p4 | p9 |
| CD31 | 98.68±0.59[a] | 0.94±0.08[b] | N.E. | 4.29±0.91[c] | N.E. |
| CD34 | 5.41±0.80[a] | 0.51±0.52[bc] | 0.30±0.32[bc] | 2.72±1.94[ac] | 0.29±0.39[bc] |
| CD45 | 0.36±0.55 | 0.16±0.09 | 0.55±0.26 | 2.12±1.69 | 0.67±0.24 |
| CD73 | 99.03±0.04[a] | 98.55±0.91[a] | 98.65±0.63[a] | 93.93±8.93[ab] | 97.79±0.76[b] |
| CD90 | 0.66±0.30[a] | 94.65±1.36[b] | 97.44±2.21[b] | 81.63±18.13[b] | 96.50±0.19[b] |
| CD105 | 98.97±0.9 | 99.71±0.15 | 98.38±1.62 | 97.85±1.47 | 92.08±6.42 |
| CD29 | 97.42±0.5[a] | 99.18±0.48[b] | 95.69±3.4[ab] | 99.41±0.47[b] | 99.15±0.21[b] |
| CD49e | 95.36±1.5[a] | 99.72±0.27[b] | 98.53±0.5[c] | 99.24±0.68[b] | 94.93±0.09[a] |
| CD166 | 1.74±0.20[a] | 92.59±2.50[b] | 71.01±1.23[c] | 77.29±13.86[bc] | 92.89±2.59[b] |

**Figure 3.** Immunophenotypic characterization of MSCs derived from human iPS cells cultured on poly[2-(methacryloyloxy)ethyl dimethyl-(3-sulfopropyl)ammonium hydroxide]. **(A):** Representative dot-plots showing the expression of cell surface markers present or absent on derived human iPS-MSCs at passage 4. Refer to negative expression in the lower left gate, while positive expression is illustrated in the lower-right gate. **(B):** Table showing the expression of cell surface markers on derived human iPS-MSCs at passage (P) 1, 4, and 9 compared to hBMSCs and HUVEC as positive and negative controls, respectively. Data are presented as the mean ± SD, and values with different letters indicate statistically significant ($p < .05$) differences. For representative dot-plots histograms of hBMSC and HUVEC refer to supporting information Figure 2. N.E. indicates not evaluated. Abbreviations: hBMSC, human bone marrow stroma cells; hiPS-MSCs, human-induced pluripotent stem-derived mesenchymal stem cells; HUVEC, human vascular endothelial cells.

Selected colonies were collected to form EBs, while other colonies were maintained on PMEDSAH-coated plates for further propagation as undifferentiated iPSCs. Initially, a heterogeneous cell population developed from EBs and by passage 2, greater than 90% of the total cell population acquired a fibroblast-like morphology that matched the described morphology of derived hES-MSCs [4, 5]. As an initial characterization to confirm the derivation of MSCs from the iPSCs, FACS analysis of cell surface markers present in human bone marrow stromal cells (hBMSC) was performed at passages 1, 4, and 9 (Fig. 3). The immunophenotype of the iPS-MSCs was similar to hBMSCs (supporting information Fig. 2A) and consistent over all time points studied, showing high expression (>90%) for CD73, CD90, CD105, CD29, CD49e, and CD166, while exhibiting low expression (<3%) for CD34 and CD45. The expression of CD31 on the iPS-MSCs was also analyzed and compared to human vascular endothelial cells (4.3% vs. 99.1%, respectively; supporting information Fig. 2B). Messenger RNA analysis by qRT-PCR demonstrated that *Oct3/4, Sox2*, and *Nanog* expression was downregulated in the derived iPS-MSCs relative to parental hiPSCs (supporting information Table 2). Similarly, the expression of *c-Myc* and *Klf4*, used in the reprogramming of human fibroblasts into iPSCs, was downregulated in the derived iPS-MSCs. The derived iPS-MSCs maintained a normal karyotype over 12 passages (supporting information Fig. 1B) and were able to form colonies after seeding at clonogenic concentrations (supporting information Fig. 3A). The cell doubling time of this population was calculated to be approximately 23 hours (supporting information Fig. 3B).

To verify the multilineage differentiation capacity of the iPS-MSCs in vitro, cells were directed to differentiate toward adipogenic, chondrogenic, and osteogenic lineages. Adipogenic differentiation of iPS-MSCs was demonstrated by a fivefold increase in peroxisome proliferators-activated receptor gamma (*PPAR-γ*) mRNA in iPS-MSCs treated with adipogenic factors as compared to controls (supporting information Fig. 4). Chondrogenic differentiation was observed after iPS-MSCs were cultured as micromass pellets in medium containing chondrogenic supplements for 4 weeks. Safranin O staining of chondrogenic pellets revealed chondrocyte-like cells residing in lacunae surrounded by a well-defined glycosaminoglycan (sGAG) and proteoglycan-rich extracellular matrix (Fig. 4A). qRT-PCR analysis of chondrogenic pellets demonstrated a significant ($p < .05$) increase in mRNA levels for genes related to chondrogenesis, such as aggrecan (*ACAN*), and collagen type II alpha 1 (*COL2A1*), while no significant ($p > .05$) increases were observed for other related genes such as perlecan [also known as heparan sulfate proteoglycan 2 (*HSPG2*)], glypican 3, and syndecan 2 (*SDC2*) when compared with iPS-MSCs cultured in 2D with growth medium (Fig. 4B).

Osteogenic differentiation of iPS-MSCs was induced after cells were cultured in medium containing osteogenic supplements for 4 weeks. By the end of the differentiation assay, calcium deposition was observed in iPS-MSCs cultured with

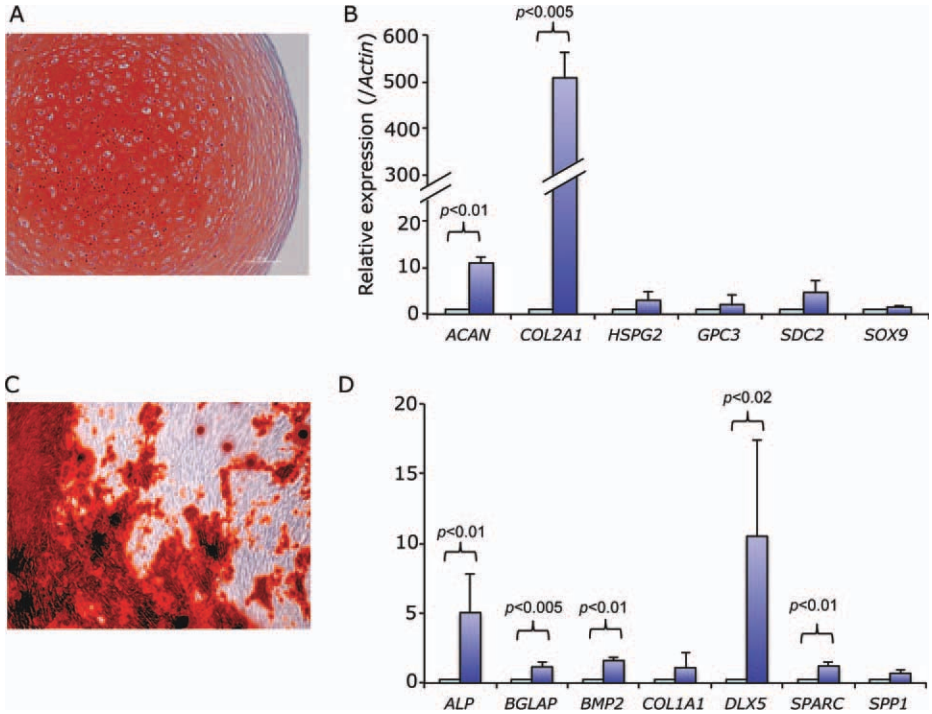


**Figure 4.** In vitro differentiation of human-induced pluripotent stem cell-derived mesenchymal stem cells. **(A):** Chondrogenic differentiation confirmed by histology and Safranin "O" staining and **(B)** upregulation of chondrogenic-related genes. **(C):** Osteogenic differentiation confirmed by Alizarin Red staining and **(D)** upregulation of osteogenic-related genes. Quantitative real-time PCR data (mean ± SD) normalized to human *β-Actin* expression from differentiated cells (dark blue columns) compared to control cells (light blue columns). Abbreviations: *ACAN*, aggrecan; *ALP*, alkaline phosphatase; *BGLAP*, osteocalcin; *BMP2*, bone morphogenic protein 2; *COL1A1*, collagen type I alpha 1; *COL2A1*, collagen type II alpha 1; *DLX5*, distal-less homeobox 5; *GPC3*, glypican 3; *HSPG2*, perlecan; *SDC2*, syndecan 2; *SPP1*, bone sialoprotein 1.

osteogenic medium (Fig. 4C), while matrix mineralization was not observed in cells in growth medium. In addition, qRT-PCR analysis detected significant ($p < .05$) increases in mRNA levels of genes related to osteogenesis such as bone morphogenic protein 2 (*BMP2*), osteocalcin (also known as bone gamma-carboxyglutamic acid-containing protein): (*BGLAP*), ALP, osteonectin (*SPARC*), and distal-less homeobox 5 (*DLX5*) in mineralized iPS-MSCs, while no significant ($p > .05$) increases were noted for collagen type I alpha 1 (*COL1A1*) and bone sialoprotein 1 compared to proliferating iPS-MSCs (control group) (Fig. 4D). To demonstrate the specificity of iPS-MSC commitment under defined culture conditions, the expression of genes related to chondrogenesis was evaluated in iPS-MSCs directed to osteogenesis, and vice versa. The expression of chondrogenic-related genes such as *ACAN*, *COL2A1*, and *HSPG2* was significantly ($p < .05$) lower in osteogenic samples in relation to iPS-MSCs in growth medium (supporting information Table 3). In contrast, a significant ($p < .05$) increase in expression of bone-related genes *DLX5*, *SPARC*, and *SSP1* was observed in chondrogenic samples, while a significant ($p < .05$) reduction was observed for *BGLAP* and *BMP2* compared to control iPS-MSCs.

### In Vivo Osteogenic Potential of MSCs Derived from Human iPSCs Cultured on PMEDSAH

To verify the capability of hiPS-MSCs to regenerate bone in vivo, cells treated with osteogenic medium for 4 days were transplanted into calvarial defects in immunocompromised mice. After 8 weeks, animals were euthanized and specimens were analyzed by microCT and histology. MicroCT analysis demonstrated a 4.2-fold increase in volume of new bone formed in calvariae transplanted with iPS-MSCs compared to controls (supporting information Fig. 5). New bone formation was observed within the central region and on the margins of the defect adjacent to the mouse calvaria. Histological evaluation identified osteocytes surrounded by matrix consistent with woven bone, osteoblasts lining the exterior of the newly formed bone as well as small bone marrow cavities within the newly formed bone (Fig. 5A). Fibrous connective tissue filled the rest of the defect.

To determine the contribution of the transplanted hiPS-MSCs in new bone formation, specific anti-human mAbs that do not cross-react with murine cells were used. Positive staining for both human nuclear antigen and human mitochondria was observed in osteocytes embedded in the newly formed bone but not in the native mouse bone at the surgical margins or in the fibrous tissue that filled the defect (Fig. 5B-D).

## Discussion

The use of MSCs in regenerative medicine has advanced significantly, as demonstrated by several phase I and phase II stem cell-based clinical trials (www.clinicaltrials.gov) designed to treat human conditions, such as bone defects, wound repair, myocardial infarction, stroke, diabetes, and graft-versus-host-disease [25]. While MSCs can be isolated from several human tissues, the cell-harvesting procedures are invasive, expensive, and laborious. Furthermore, the in vitro expansion capacity of isolated MSCs is limited and extensively cultured primary cells may take on phenotypic characteristics that are not consistent with the behavior of natural MSCs in vivo. Thus, iPS-MSCs represent an important alternative to primary cells. iPSCs have gained attention because they possess pluripotency, self-renewal, and differentiation properties that are similar to hESCs without sharing many of the ethical concerns associated with hESCs. However, current

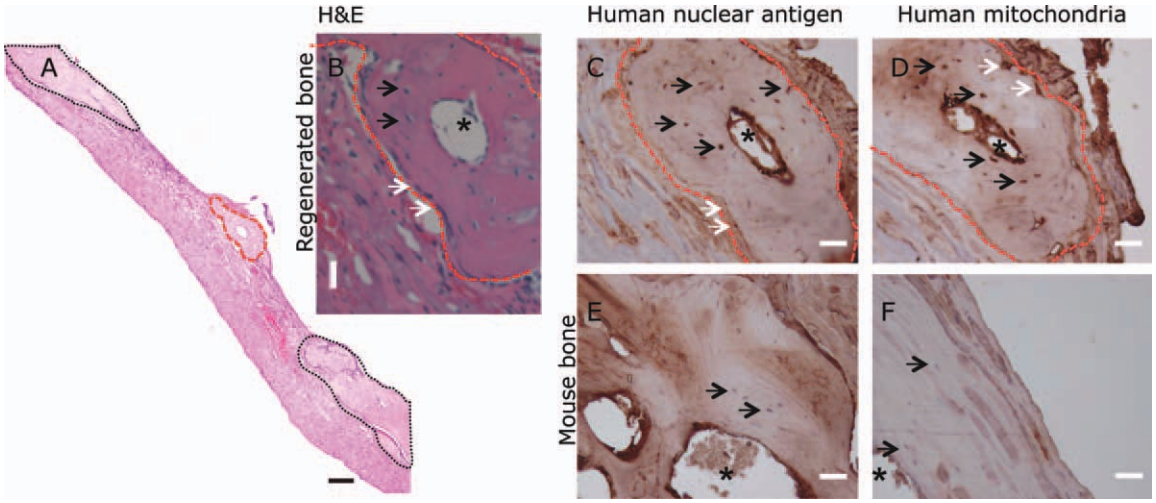


**Figure 5.** In vivo bone formation by human-induced pluripotent stem cell-derived mesenchymal stem cells (hiPS-MSCs). **(A):** H&E image of a severe combined immunodeficiency (SCID)-mouse skull section where a calvarial defect was created and hiPS-MSCs were transplanted. The limits of the mouse skull are delineated by black dashed lines (expanded in **E,F**). The red dashed line (expanded in **B–D**) indicates new-formed bone areas with osteocytes (black arrows) surrounded by matrix consistent with woven bone, osteoblasts (white arrows) lining the exterior of the newly formed bone as well as small bone marrow cavities (indicated by asterisks) within the newly formed bone. Positive immunoreactivity to human nuclear antigen (C) and human mitochondria (D) antibodies of osteocytes within the newly formed bone, while negative in the mouse bone (E and F) suggest the human origin of the regenerated bone. Scale bar in A = 100 $\mu$m, while in B–F = 20 $\mu$m.

practices to maintain hiPSCs and hESCs in an undifferentiated state typically rely on undefined and xenogeneic components that ultimately impede our ability to use these stem cells to treat debilitating human diseases.

Here, we demonstrated that hiPSCs proliferate in an undifferentiated state on PMEDSAH-coated plates, a synthetic polymer coating devoid of xenogeneic contamination. The cells could subsequently be differentiated into functional MSCs with in vivo bone formation capabilities. PMEDSAH-coated plates supported the expansion of undifferentiated hiPSCs. After 15 passages on PMEDSAH-coated plates, iPSCs maintained the expression of transcription factors and cell surface markers associated with pluripotent stem cells as well as an undifferentiated cell/colony morphology and a normal karyotype [3]. Most importantly, iPSCs cultured on PMEDSAH maintained their pluripotent character. Thus, PMEDSAH-coated culture substrates in combination with hCCM represent a clinical-grade culture system free of xenogeneic contamination for the expansion of hiPSCs. Although not a particular goal of this work, it will be important to determine whether virus-free and transgene-free iPSCs can be derived on PMEDSAH-coated plates.

Going beyond the current state-of-the-art [6], hiPSCs cultured on the fully synthetic PMEDSAH substrate under clinically compliant conditions were used to derive MSCs and transplanted in vivo where they not only survived but contributed to de novo bone formation. The derived iPS-MSCs expressed similar levels of markers present in hMSCs [26], while qRT-PCR revealed that genes associated with pluripotency and reprogramming markers were no longer expressed once the cells were directed to differentiate. This fact, coupled with the critical observation that no teratomas were formed in mice treated with transplanted hiPS-MSCs, indicated a reduced tumorigenic risk of this progenitor population compared to undifferentiated iPSCs. The derived hiPS-MSCs were able to differentiate in vitro into adipogenic, chondrogenic, and osteogenic lineages. Interestingly, the chondrogenic and osteogenic differentiation of the derived hiPS-MSCs were more pronounced than adipogenic differentiation. Similar observations have been made for different populations of derived MSCs indicating a variability that depends on the origin of the cell population [27, 28]. It remains to be determined whether the differences in differentiation levels are inherent to the nature of the derived iPS-MSCs or influenced by the origin of the parental iPSCs as dermal fibroblasts. In fact, epigenetic memory has been suggested to influence iPSC differentiation depending on their origin [8, 29, 30]. However, a significant upregulation of *PPAR-γ* in cultures treated with adipogenic medium does suggest the potential for iPS-MSC differentiation toward adipogenesis. In addition, effective chondrogenic differentiation of hiPS-MSCs was achieved, as confirmed by histological and gene expression analyses of chondrogenic micromass pellets. Robust deposition of proteoglycans was observed in pellets of iPS-MSCs treated with chondrogenic factors, as indicated by the intensity of the Safranin O staining. Significant expression of extracellular matrix-related genes present in cartilage suggests the maturity of the chondrogenic pellets obtained from hiPS-MSCs. The in vitro osteogenic differentiation of hiPS-MSCs was also robust, as demonstrated by calcium deposition and upregulation of genes related to osteogenesis in cultures treated with osteogenic medium. Taken together, the derived hiPS-MSCs described here meet the specifications of a defined MSC population, as proposed by the International Society for Cellular Therapy [31]: (a) adherence to tissue culture plastic under standard culture conditions; (b) an immunophenotype similar to that of human bone marrow stromal cells with low expression of hematopoietic stem cell (HSC) markers; and (c) the ability to undergo in vitro differentiation along the osteogenic, chondrogenic, and adipogenic lineages.

To examine the possible use of derived hiPS-MSCs in cell therapies and regenerative medicine, cell-transplantation assays were performed in immunocompromised mice with the goal of developing bone in vivo. Histological and microCT image reconstruction confirmed the formation of new bone within the calvarial defects of mice treated with transplanted hiPS-MSCs after 8 weeks. Randomly distributed and unorganized bone fragments that supported hematopoiesis were found within the calvarial defects. Furthermore, positive immunostaining of osteoblasts and osteocytes with mAbs to human nuclei and human mitochondria confirmed the participation of

transplanted hiPS-MSCs in the newly formed bone. Although the clinical critical size defect was not completely healed, the fact that hiPS-MSCs participated in bone regeneration in vivo in a calvarial defect mouse model suggests these cells became functional MSCs and osteoprogenitors that can be used as a tool for future cell-transplantation studies that investigate bone regeneration in response to disease, trauma, or congenital anomalies. Future work investigating factors such as the ideal number of transplanted cells, survival and distribution, in vitro osteogenic induction prior to transplantation, and the optimal biomaterial scaffold with osteoconductive properties is necessary to determine the role that transplanted cells may play in regenerating significant skeletal lesions.

## Conclusions

In summary, undifferentiated hiPSCs can be cultured on the synthetic polymer coating, PMEDSAH, in xeno-free conditions. iPSCs maintained on this substrate have the capacity to differentiate into functional MSCs both in vitro and in vivo. Taken together, the PMEDSAH culture system and efficient iPS-MSC derivation on this synthetic substrate provides a unique platform for the future design of cell-based strategies for tissue regeneration.

## Acknowledgments

We thank William King for his insightful comments and critical reading of the manuscript, Sun Hongli, Michael Pressler, and Michelle. Lynch and Marta Dzaman for their support performing surgical procedure and cell transplantation in craniofacial defect model, qRT-PCR, microCT analysis, and immunohistochemistry, respectively. This research was supported by the NIH Grants R01 DE016530, R01 NS065450, F31 DE019760 and the NIDCR T32 Tissue Engineering and Regeneration Training Program.

## Disclosure of Potential Conflicts of Interest

The authors indicate no potential conflicts of interest.

## References

1 Takahashi K, Tanabe K, Ohnuki M et al. Induction of pluripotent stem cells from adult human fibroblasts by defined factors. Cell 2007; 131:861–872.
2 Takahashi K, Yamanaka S. Induction of pluripotent stem cells from mouse embryonic and adult fibroblast cultures by defined factors. Cell 2006;126:663–676.
3 Thomson JA, Itskovitz-Eldor J, Shapiro SS et al. Embryonic stem cell lines derived from human blastocysts. Science 1998;282:1145–1147.
4 Lian Q, Lye E, Suan Yeo K et al. Derivation of clinically compliant MSCs from CD105+, CD24− differentiated human ESCs Stem Cells 2007;25:425–436.
5 Brown SE, Tong W, Krebsbach PH. The derivation of mesenchymal stem cells from human embryonic stem cells. Cells Tissues Organs 2009;189:256–260.
6 Lian Q, Zhang Y, Zhang J et al. Functional mesenchymal stem cells derived from human induced pluripotent stem cells attenuate limb ischemia in mice. Circulation 2010;121:1113–1123.
7 Ozawa K, Sato K, Oh I et al. Cell and gene therapy using mesenchymal stem cells (MSCs). J Autoimmun 2008;30:121–127.
8 Pittenger MF, Mackay AM, Beck SC et al. Multilineage potential of adult human mesenchymal stem cells. Science 1999;284:143–147.
9 Katz AJ, Tholpady A, Tholpady SS et al. Cell surface and transcriptional characterization of human adipose-derived adherent stromal (hADAS) cells. Stem Cells 2005;23:412–423.
10 Bianco P, Riminucci M, Gronthos S et al. Bone marrow stromal stem cells: Nature, biology, and potential applications. Stem Cells 2001;19:180–192.
11 Bieback K, Kern S, Kluter H et al. Critical parameters for the isolation of mesenchymal stem cells from umbilical cord blood. Stem Cells 2004;22:625–634.
12 Romanov YA, Svintsitskaya VA, Smirnov VN. Searching for alternative sources of postnatal human mesenchymal stem cells: Candidate MSC-like cells from umbilical cord. Stem Cells 2003;21:105–110.
13 Igura K, Zhang X, Takahashi K et al. Isolation and characterization of mesenchymal progenitor cells from chorionic villi of human placenta. Cytotherapy 2004;6:543–553.
14 Richards M, Fong CY, Chan WK et al. Human feeders support prolonged undifferentiated growth of human inner cell masses and embryonic stem cells. Nat Biotechnol 2002;20:933–936.
15 Nagaoka M, Si-Tayeb K, Akaike T et al. Culture of human pluripotent stem cells using completely defined conditions on a recombinant E-cadherin substratum. BMC Dev Biol 2010;10:60.
16 Rodin S, Domogatskaya A, Strom S et al. Long-term self-renewal of human pluripotent stem cells on human recombinant laminin-511. Nat Biotechnol 2010;28:611–615.
17 Brafman DA, Chang CW, Fernandez A et al. Long-term human pluripotent stem cell self-renewal on synthetic polymer surfaces. Biomaterials 2010;31:9135–9144.
18 Klim JR, Li L, Wrighton PJ et al. A defined glycosaminoglycan-binding substratum for human pluripotent stem cells. Nat Methods 2010;7:989–994.
19 Melkoumian Z, Weber JL, Weber DM et al. Synthetic peptide-acrylate surfaces for long-term self-renewal and cardiomyocyte differentiation of human embryonic stem cells. Nat Biotechnol 2010;28:606–610.
20 Villa-Diaz LG, Nandivada H, Ding J et al. Synthetic polymer coatings for long-term growth of human embryonic stem cells. Nat Biotechnol 2010;28:581–583.
21 Huebsch N, Gilbert M, Healy K. Analysis of sterilization protocols for peptide-modified hydrogels. J Biomed Mater Res Part B: Appl Biomater 2005;74B:440–447.
22 Hentschel J, Ten Cate MGJ, Borner HG. Peptide-guided organization of peptide-polymer conjugates: Expanding the approach from oligo- to polymers. Macromolecules 2007;40:9224–9232.
23 Nandivada H, Villa-Diaz LG, O'Shea KS et al. Fabrication of synthetic polymer coatings and their use in feeder-free culture of human embryonic stem cells. Nat Protoc 2011;6:1037–1043.
24 Schmittgen TD, Livak KJ. Analyzing real-time PCR data by the comparative C(T) method. Nat Protoc 2008;3:1101–1108.
25 Bernardo ME, Pagliara D, Locatelli F. Mesenchymal stromal cell therapy: A revolution in regenerative medicine? Bone Marrow Transplant 2012;47:164–171.
26 Majumdar MK, Keane-Moore M, Buyaner D et al. Characterization and functionality of cell surface molecules on human mesenchymal stem cells. J Biomed Sci 2003;10:228–241.
27 Kaltz N, Funari A, Hippauf S et al. In vivo osteoprogenitor potency of human stromal cells from different tissues does not correlate with expression of POU5F1 or its pseudogenes. Stem Cells 2008;26:2419–2424.
28 Zhao L, Li G, Chan KM et al. Comparison of multipotent differentiation potentials of murine primary bone marrow stromal cells and mesenchymal stem cell line C3H10T1/2. Calcif Tissue Int 2009;84:56–64.
29 Kim K, Doi A, Wen B et al. Epigenetic memory in induced pluripotent stem cells. Nature 2010;467:285–290.
30 Polo JM, Liu S, Figueroa ME et al. Cell type of origin influences the molecular and functional properties of mouse induced pluripotent stem cells. Nat Biotechnol 2010;28:848–855.
31 Dominici M, Le Blanc K, Mueller I et al. Minimal criteria for defining multipotent mesenchymal stromal cells. The International Society for Cellular Therapy position statement. Cytotherapy 2006;8:315–317.


See www.StemCells.com for supporting information available online.